NUMERICAL MODELING OF FILM CONDENSATION USING TWO-PHASE FLOWS & ITS EFFECT ON HEAT & MASS TRANSFER

Arun K Raj, Jayakumar J.S*

Department of Mechanical Engineering

Amrita School of Engineering, Amritapuri Campus

Kollam, Kerala, Pin code: 691021

arunkraj03@gmail.com, jsjayan@am.amrita.edu

ABSTRACT

A two-phase Eulerian solver has been modeled to compute the effect of condensation heat transfer coefficient on laminar film condensation. For analysis, the solver is incorporated with void fraction, energy equations for individual phases and a set of empirical correlations to compute average heat transfer coefficient, film thickness and the amount of condensate formed. A Finite Volume Method (FVM) is used to discretize the governing equations. At a constant flow rate, the effect of film thickness and mass of condensate formed over vertical surfaces with varying temperature differences (ΔT) are studied. The result indicated that the heat transfer coefficient tends to decrease with an increase in film thickness.

Keywords: two-phase, FVM, film condensation, film thickness, heat transfer coefficient, mass of condensate

1. INTRODUCTION

Thermal interactions between condensate and the surface in contact play a vital role in predicting the performance of thermal equipment's. Regardless of the modes of condensation, the condensate layer formed over the surface creates a resistance to heat transfer. Hence, the estimation of mass of condensate formed over heat transfer surfaces becomes relevant as it can be used to estimate the resistance offered towards thermal interactions. A persistent theme throughout the study of multiphase flows is its need to model and predict the detailed behavior of such flows and the phenomena that they manifest. This paper mainly focuses on two-phase flows involving laminar film condensation over vertical surfaces. The effect of condensation heat transfer coefficient, film thickness and mass of condensate on laminar film condensation are investigated in this paper.

A simple correlation was suggested by Shah (1979) to estimate condensing heat transfer coefficient using thermodynamic vapor quality and reduced pressure (p_r) as the parameters. The correlation was verified by conducting experiments using several working fluids at a wide range of Reynolds numbers from 100- 63,000 and liquid Prandtl no's from 1-13. Experiments were conducted using horizontal, vertical and inclined tubes. An improved correlation was introduced by Shah (2009) for condensation in plane tubes, which introduced transport properties and Reynolds number into the expression. The modified correlation produced better results for turbulent and laminar flows and was in good agreement with the Nusselt's analytical solutions. The effect of interfacial shear stress on condensation heat transfer was experimentally investigated by Thumm et.al (2001). The study was extended to the use of large values of Reynolds number, to understand the effect of turbulence in heat transfer. It was concluded that as interfacial shear stress increases, the heat transfer coefficient decreases up to flow Reynolds number (Re_f) <10. In turn the heat transfer coefficient increases when Re_f was increased from 20 to 670 and at fully turbulent scenario the effects seem to be balancing each other.

An analytical model to compute the heat transfer characteristics involving laminar film-wise condensation in small diameter tubes was suggested by Wang and Du (2000). A subsequent experimental work validated the results obtained from the suggested model. The analysis showed that effect of gravity decreases in micro/mini tubes during flow condensation. The effect of inclination angles on condensation heat transfer is further analyzed. The results obtained suggested that at low vapor inlet Reynolds number and in large diameter

tubes the distribution of inclination angle enhances the heat transfer. Dalkilic et.al (2009) based on their experimentation, analyzed the effect of pressure and mass flow rates on film thickness, condensation rate and heat transfer coefficient by using R134a as the working fluid. Laminar flow analysis carried out on the vertical tube revealed that at low mass flow rates, the thickness of the condensate film formed on the tube walls are higher in comparison with film thickness obtained at higher flow rates. As a result the heat transfer coefficient was found to decrease along the tube length. This is due to the film formed over the surfaces which pose a resistance to heat transfer. Zhao and Du (2003) performed a theoretical analysis on film condensation heat transfer to study the meniscus draining effect. They used a vertical micro tube with a thin metal wire welded on its inner surface. The heat transfer characteristics are estimated based on parameters such as contact angle between the condensing wall and the condensate considering the diameter of wire. The study revealed that increase in wire diameter can enhance the heat transfer and in turn the wettability of wire and condensate has less influence of overall heat transfer characteristics. However the contact between the wire and the condensate has effects on distribution of condensate within the flow system.

A numerical model was developed by Stefano and John (2010) for laminar annular film condensation for different channel shapes. The model is based on a finite volume formulation of the Navier-Stokes and energy equations. Simulation results are obtained for isothermal, iso-heat flux and variable heat flux external wall boundary conditions. The instantaneous local and perimeter averaged heat transfer coefficients, condensate film thickness distribution, the cross sectional void fraction and the vapor quality for circular, elliptical and flower shape cross sections are obtained. The model has been validated against various bench mark and experimental results. Condensation in a capillary groove using the volume of fluid (VOF) model was investigated by Zhang and Faghri (2001). The effects of temperature drop, contact angle, surface tension and fin thickness on the condensation heat transfer are studied. The analysis shows that film thickness at the fin top is independent on convection within the liquid. In turn it was found that heat transfer is larger at the fin top surface as the thickness of film is lesser there when compared to that in meniscus. As the contact angle increases the liquid film on the fin top becomes flatter and the heat transfer coefficient on the fin top becomes more uniform. Moreover, local heat flux was found to be higher at the fin top when surface tension was increased. It was hence concluded that an increase in fin thickness will increase the thickness of liquid film.

Perflurohexane (C_6F_{14}) was used as the working fluid for experimental and numerical analysis of condensation in a vertical tube by Lee et.al (2015). Numerical computation was performed using FLUENT and was verified against the experimental data. Heat flux and wall temperature variation in axial direction was used to compute the heat transfer coefficient. The study carried out emphasized the need to model better numerical techniques to closely compute the film thickness and variations of velocity and temperatures thereby refine the two-phase computational models. Mimouni et.al (2010) model the steam condensation based on the balance of heat and mass transfer between droplets and gas mixture surrounding droplet. Two tests were performed to validate the condensation against experimental data. Predictions regarding axial velocity do not agree with certain cases as it wasn't incorporated with turbulence modeling. Vemuri and Kim (2005) experimentally and theoretically investigated the effect of condensation on heat transfer coefficient. There is an enhancement up to three times in heat transfer rate for drop wise condensation when operated at vacuum condition and an enhancement of eight times when operated at atmosphere condition over film wise condensation. One possible reason for the larger values in heat transfer rate may be due to the effect of interfacial shear stress. At atmospheric pressure its value is extremely high when compared to vaccum pressure. Phan and Narain (2007) presented numerical solutions of the 2D-governing equations for the Nusselt problem involving film condensation of quiescent saturated vapor on a vertical wall. The main focus was to understand the effects of stability, instability and wave effects during low Reynolds number flows. The study reveals the effect of instabilities in the flow during the transition from laminar to turbulent around a critical film Reynolds number of 30. In addition, the heat transfer rates can be further improved due to wave effects and can be put into application using suitable actuators.

2. MODEL DESCRIPTION

The working fluid flows into the computational domain at the top as denoted in the Fig.1. The vertical plate is maintained at a uniform temperature (T_{wall}) on either sides. The wall temperature is maintained below the saturation temperature of the incoming working fluid. The fluid flow takes place at uniform pressure (P_{in}) and uniform velocity (V_{in}) which are specified as the inlet boundary conditions. The characteristic length of the plate is denoted by L and width by w. The thickness of the condensate layer is denoted as δh_x and acceleration due to gravity by g. The boundary conditions and thermophysical properties used in the analysis are discussed in the following sections. The various assumptions made while formulating the governing equations were: (i) both the phases (liquid and gas) are assumed to be Newtonian fluids. For both phases, the shear stress is said to vary linearly with strain rate (ii) the liquid-vapor interface is assumed to be smooth (iii) the vapor is treated as an ideal gas mixture (iv) the pressure is assumed to be uniform in the radial direction (v) saturation conditions are assumed at the interface - for condensation to occur, the vapor must be saturated. Therefore the interface temperature will be equal to the saturation temperature corresponding to the partial pressure of vapor (vi) interfacial shear stresses are not considered into computation (vii) the condensate flows under the influence of gravity (g). The computational domain is as shown in Fig. 2.

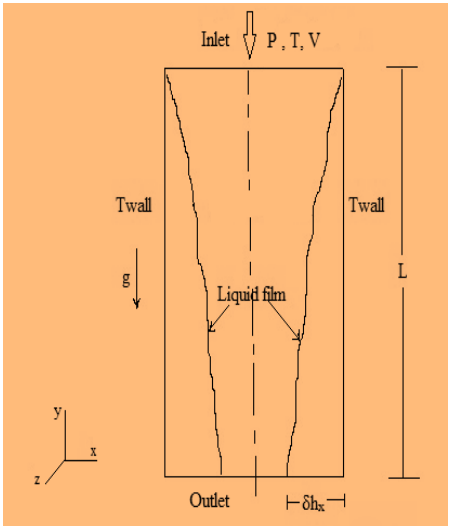

Figure1. Physical model

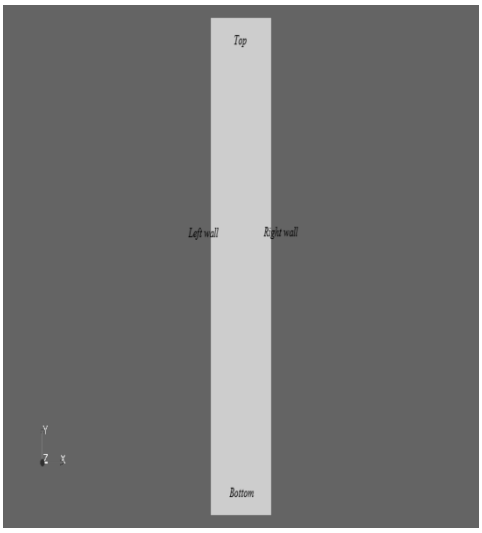

Figure2. Computational Domain

2.1 Governing Equations

Governing equations comprises of variables that govern the problem expressed in terms of differential equations. A set of two dimensional incompressible flow governing equations, based on the conservation of mass, momentum and energy for both liquid and vapour phase are as listed below

2.1a Liquid Phase Governing Equations

Liquid Continuity Equation:

$$\frac{\partial}{\partial t}(\alpha_L) + \nabla(\alpha_L V_L) = 0 \qquad (1)$$

Liquid Momentum Equation:

$$\frac{\partial}{\partial t}(\alpha_L V_L) + \nabla(\alpha_L V_L V_L) = -\alpha_L \nabla p + \alpha_L g \quad (2)$$

Liquid Energy Equation:

$$\frac{\partial}{\partial t}(h_L) + \nabla(V_L h_L) = \nabla(k_{eff,L}\, \nabla h_L) \quad (3)$$

2.2b Vapor Phase Governing Equation

Similar to liquid phase, vapor phase is also governed by equations of mass, momentum and energy.

Vapor Continuity Equation:

$$\frac{\partial}{\partial t}(\alpha_g) + \nabla(\alpha_g V_g) = 0 \quad (4)$$

Vapor Momentum Equation:

$$\frac{\partial}{\partial t}(\alpha_g V_g) + \nabla(\alpha_g V_g V_g) = -\alpha_g \nabla p + \alpha_g g \quad (5)$$

Vapor Energy Equation:

$$\frac{\partial}{\partial t}(h_g) + \nabla(V_g h_g) = \nabla(k_{eff,g}\, \nabla h_g) \quad (6)$$

2.2 Correlations

In laminar flow analysis, to compute the variations of heat transfer coefficient, boundary layer thickness and mass of condensate formed for a particular flow rate, various correlations has been incorporated in the solver '*laminarFilmCondensationFoam*'. To analyze laminar flow, the empirical relations used are based on Nusselt theory. These equations are listed from Eqns. (7) – (10) as follows:

(a) Average heat transfer coefficient (h_{avg})

$$h_{avg} = 0.943 * \sqrt[0.25]{\frac{K_f{}^3 * \rho_f(\rho_f - \rho_v) * g * h_{fg}}{\mu_f * L * \Delta T}} \quad (7)$$

(b) Nusselt Number (Nu)

$$\mathrm{Nu} = \frac{h_{avg} * \mathrm{L}}{K_f} \quad (8)$$

(c) Boundary layer thickness (δh_x)

$$\delta h_x = \sqrt[0.25]{\frac{4 * K_f * \mu_f * x * \Delta T}{\rho_f(\rho_f - \rho_v) * g * h_{fg}}} \quad (9)$$

(d) Mass of condensate formed ($\dot{m}$)

$$\dot{m} = \frac{\rho_f(\rho_f - \rho_v) * g}{3 * \mu_f} * \delta h_x{}^3 \quad (10)$$

2.3 Boundary conditions

The initial and boundary conditions are specified based on the nature of flow, geometry of the model and governing parameters used for the analysis. For validation purposes, the working fluid used was Perflurohexane (vapor) which flows into the domain (vertical plate) at a constant velocity and at a constant inlet temperature of 359.6K. The walls of the plate are maintained at 295.3K. The thermo physical properties and values of constants are assigned based on the experimental inputs suggested by Lee et. al (2015). On the other hand, the study was carried out using steam as the working fluid. The inlet temperature of the steam was set at 373K and the wall temperature was held constant. The temperature of the wall was assigned based on the temperature difference between film and the vapor. At 20K and 40K temperature difference (ΔT) between condensing film and vapor, the analysis was performed. The phase fraction of vapor was set to 1 in both cases. In each case during film condensation, the dependence on wall temperature and the variation of heat transfer coefficient is analyzed. The analysis are also carried out at Reynolds numbers ranging from 10-1000 (laminar flow). The Reynolds number was computed by using the basic relationship between characteristic length (L), velocity (V) and kinematic viscosity (υ). The condensate thus formed flows under the influence of gravity and is laminar. The transport properties & thermo physical properties of steam and water were obtained from Kothandaraman (2010).

3. NUMERICAL SOLUTION

The CFD computational tool, OpenFOAM contains a set of numerical tools and methods to solve problems related with engineering applications such as heat transfer and fluid flows. Foremost, OpenFOAM design is relevant with the solver applications, written using the OpenFOAM classes, having a syntax that closely resembles to the partial differential equations being solved. In this study, the matter is represented as continuum and a Finite Volume Method (FVM) is used to discretize the governing equations stated in the problem. Often FVM discretize the transport equations into a matrix algorithm which is applied to all arbitrary shaped cells (any number of faces/ any number of edges) within the computational domain to obtain desired results. A two-phase Eulerian solver (OpenFOAM: version 2.2.2) is modified to account for energy interactions between the phases as mentioned by Eq. (2.3) & Eq. (2.6). The void fraction or phase fraction (α) denotes the distribution of each phase in a cell volume. The mass of vapor condensing into liquid is assumed to be conserved. The effect of average heat transfer coefficient and mass of condensate formed at the cold wall surface due to laminar film condensation is evaluated by using the Eq. (2.7) – Eq. (2.10). The working loop of the modified solver '*laminarFilmCondensationFoam*' is briefly explained here.

The solver is entirely based on PIMPLE algorithm. The steady-state and transient terms are solved using a semi-implicit method based on pressure-linked equation i.e. PISO-SIMPLE (PIMPLE) algorithm. The Navier-Stoke's equation is coupled with iterative procedure in SIMPLE algorithm, which calculates pressure from the velocity components specified in the grid. The PIMPLE algorithm then combines the SIMPLE algorithm and uses pressure implicit with splitting the operators (PISO) algorithm to rectify the second pressure correction and correct both velocities and pressure explicitly. Turbulence parameters are not taken into consideration in the modified solver. The run-time discretization schemes in OpenFOAM were used to be discretized using Gaussian integration and flux interpolation schemes. In our analysis, the convective (divergence) terms and diffusive (laplacian) terms are solved by using Gauss limited linear schemes and unbounded second order Gauss linear corrected schemes. First order, bounded, implicit Eulerian schemes are used to solve transient terms. The variation of pressure is numerically computed using generalized geometric-algebraic multi-grid (GAMG) and a smoother Diagonal incomplete-Cholesky (DIC). Preconditioned bi-conjugate gradient (PBiCG) were used to discretize enthalpy terms and the phase fraction alpha is solved by using preconditioned conjugate gradient (PCG) solver. In transient simulations, it is usual to set the solver relative tolerance to 0 to force the solution to converge to the solver tolerance in each time step. Relaxation factor and relative tolerance are set for velocity, pressure and alpha as 1 and 0.1 respectively.

3.1 Comparison of numerical results with experimental study

In order to ensure the numerical results obtained from the solver '*laminarFilmCondensationFoam*' were accurate, a validation test with the experimental work of Lee et. al (2015) was carried out. For validating the solver the working fluid chosen was Perflurohexane (C_6F_{14}) or FC-72. The experimental setup consists of a primary loop for FC-72 and two secondary water loops. Heat transfer adequate for condensation is achieved using these water loops via a condensation module. A gear pump is used to pump the working fluid (liquid) which is subsequently heated by using a pre-heater (14.2kW) by which the liquid FC-72 is converted to vapor. It is then passed on to the condensation module where a counter-flow of first water loop section is located. From the condensation module, FC-72 enters a plate type condenser where it is cooled by the second water cooling loop. An air-cooled condenser located at the exit end of plat type condenser ensures that any vapor exiting the test module is in sub-cooled liquid state before returning to the primary loop's reservoir. The computational domain was of 0.012 x 0.8m in dimensions. A grid independency test was performed using various mesh sizes of 400x400x1, 600x600x1, 700x700x1 and 800x800x1. The results of grid dependency study are as shown in Fig. 3. The wall temperature variation along the length of flow is compared at various mesh sizes. The results obtained showed that there is no difference between 700x700x1 & 800x800x1 grid system. Hence mesh size of 700x700x1 was selected as the optimum number of mesh elements for validation.

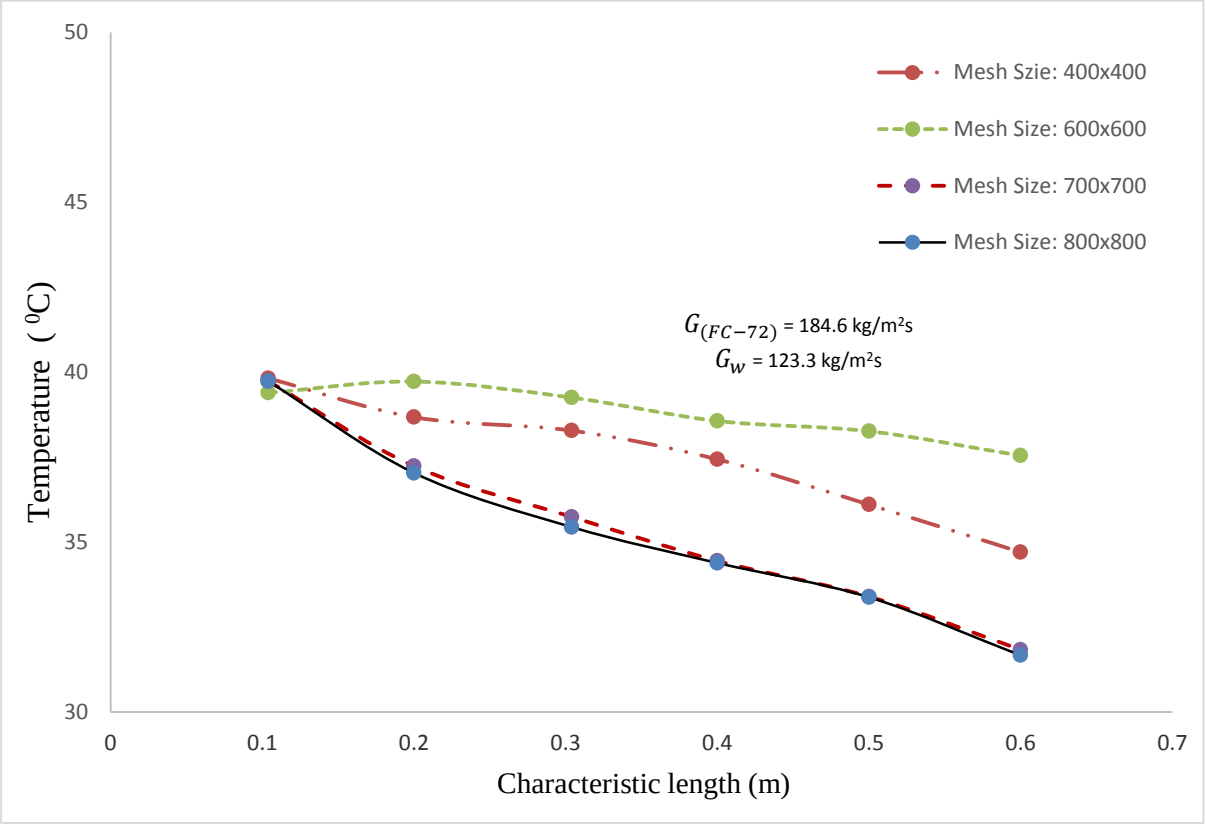

Figure 3. Grid independency test

At two different flow rates of FC-72 and water, the experimental study was conducted and is then compared with OpenFOAM results as shown in Fig. 4. The temperature of water flowing through the condensing water loop was maintained at 295.3K for all of the cases. Hence the wall temperature is held constant. At first, FC-72 with $G_{(FC-72)}$= 184.6kg/m^{2}s and water with G_w= 123.3 kg/m^{2}s flow rates was studied. The analysis shows

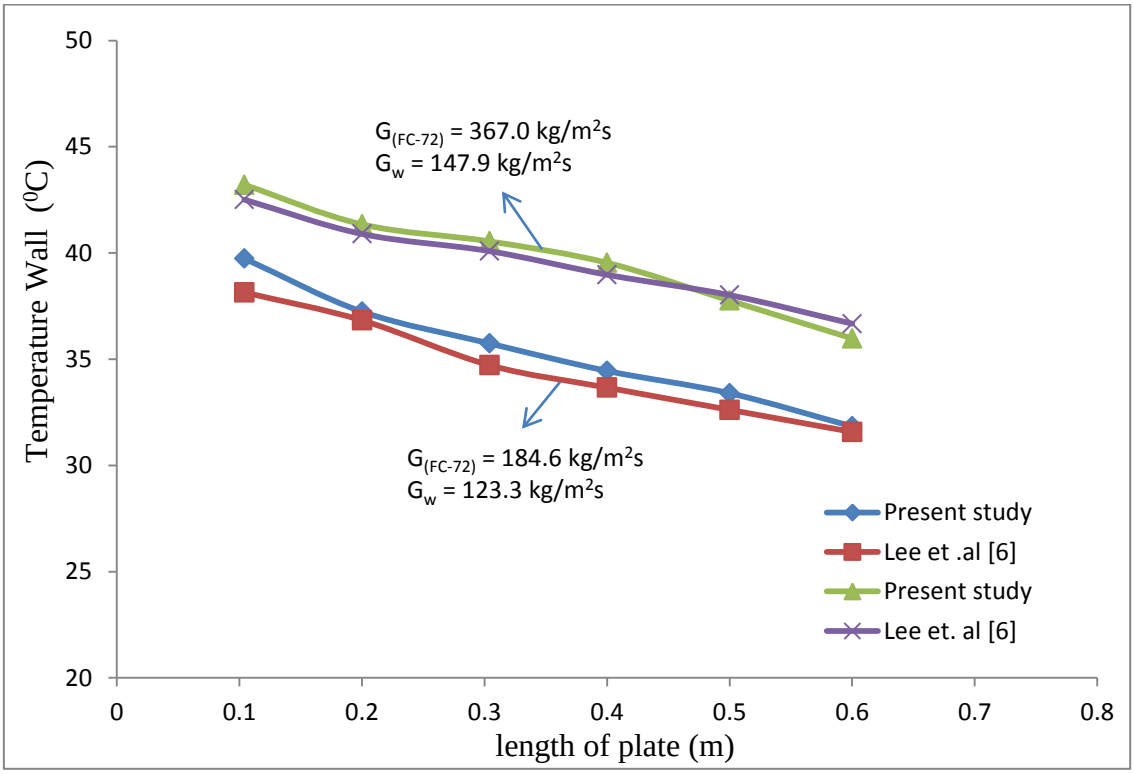

Figure 4. Comparison of experiment values with OpenFOAM

that the temperature of the vapor drops due to formation of liquid (FC-72) film on the wall surface. When the vapor flows in through the inlet, it interacts with the cold wall surface maintained at a temperature below T_{sat} of the working fluid. Due to thermal interactions between cold wall and vapor the process of condensation is initiated. The condensate thus formed flows downward under the influence of gravity thereby blanketing the wall surface. The film thus acts as a resistance to heat transfer. The variation of heat transfer coefficient and mass of condensate formed due to laminar film condensation will be explained in the subsequent sections.

4. RESULTS & DISCUSSION

Pure steam is the working fluid, which is made to flow over a vertical plate of dimension 10mm x 50mm and the entire geometry consisted of around 40,000 elements. The meshing was uniform throughout the domain. The inlet temperature of the steam was set at 373K and the wall temperature was held constant. At 20K and 40K temperature difference (ΔT) between condensing film and vapor, the analysis was performed. In each case during film condensation, the dependence on wall temperature and the variation of heat transfer coefficient is analyzed.

In Figure 5. the variation of alpha (phase/void fraction) at different time intervals are as shown. Initally at the inlet, the phase fraction of steam flowing into the domain was set to 1. The wall is specified with no-slip boundary condition. When the vapor flows over the plate surface due to temperature difference (ΔT) between wall and the incoming vapor, heat transfer takes place. The thermal interactions kick start the condensation phenomenon thereby, it results in the formation of condensate on the surafce of the wall which flows downward under the influence of gravity. As steam continuously flows over the surface, the thickness of the condensate layer keeps increasing propotionally with condensation rate as shown in Fig. 5. By using this variation in alpha, the amount of liquid film formed on wall surfaces can be estimated.

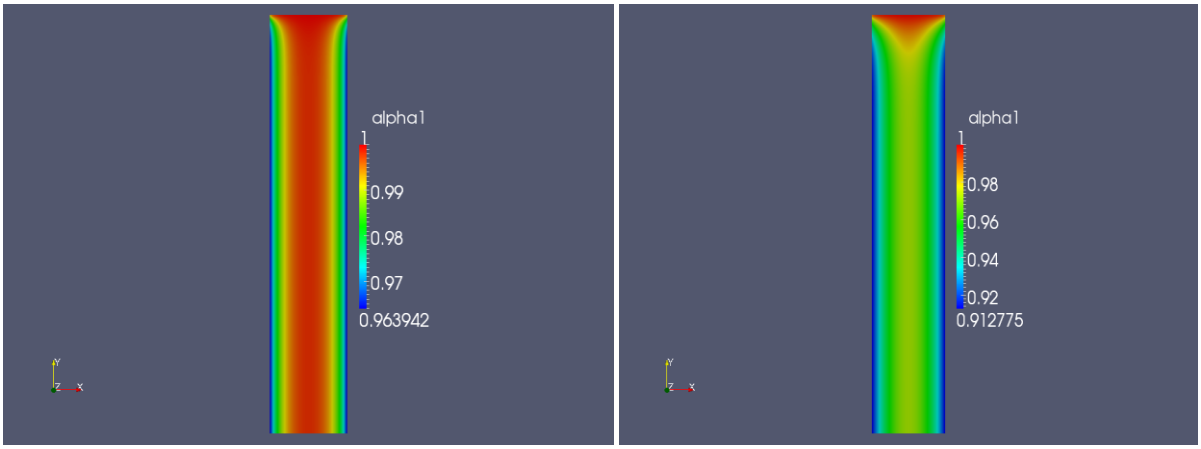

(a). variation at t= 0.1s **(b). variation at t= 0.5s**

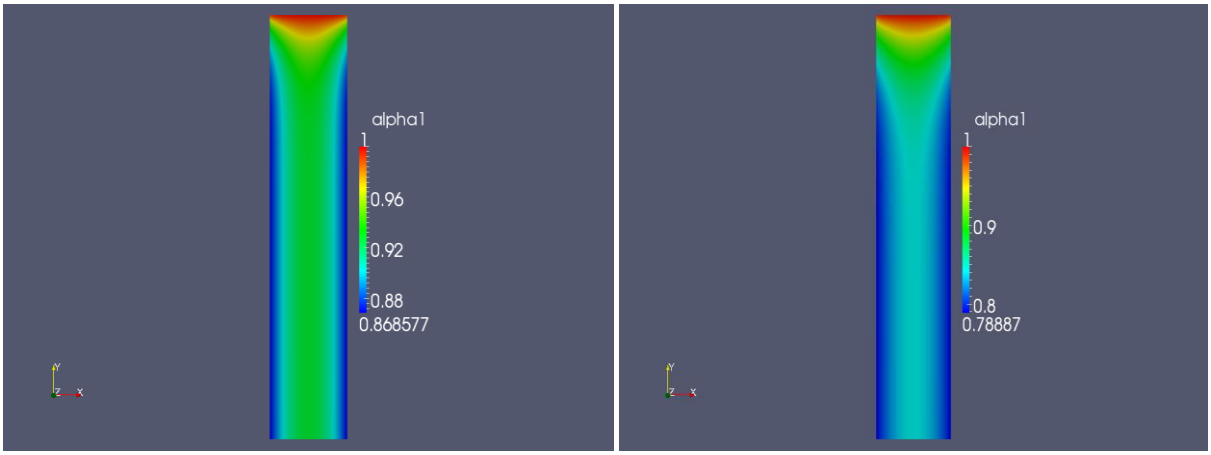

(c). variation at t= 1s **(d). variation at t= 2s**

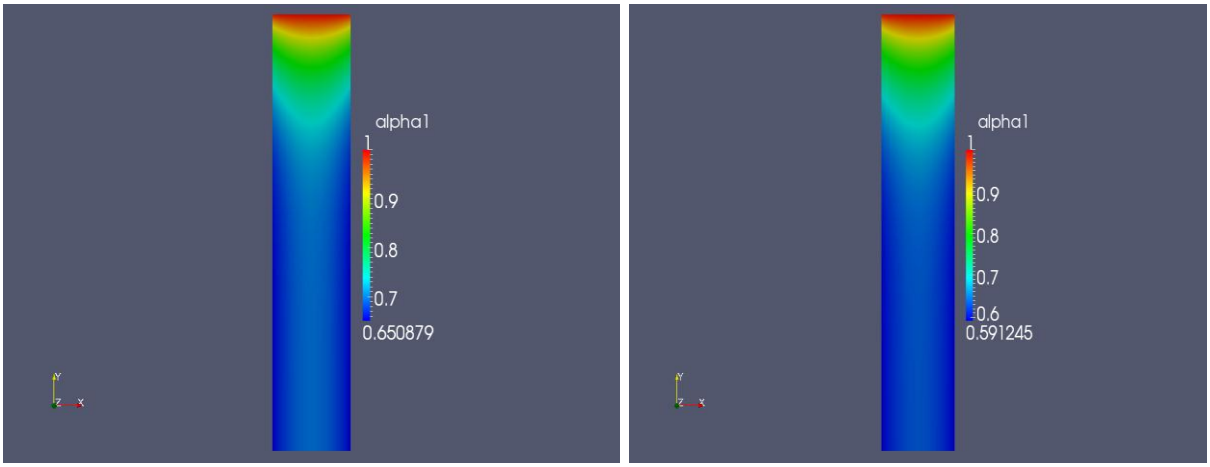

(e). variation at t= 4s **(f). variation at t= 5s**

Figure 5. Variation of phase fraction at various time intervals

The heat transfer coefficient is computed using Nusselt theory for laminar flow as mentioned in section 2.3. At a constant flow rate (Re 1000), the variation of average heat transfer coefficient at various temperature difference (ΔT) is plotted against the length of plate which is as shown in Fig.6. Condensation process is initiated due to energy interaction between the incoming vapor at a higher enthalpy and the cold wall maintained at a lower enthalpy (below the vapor saturation enthalpy). This energy interaction leads to a change of phase resulting in the formation of a layer of liquid film on the cold wall surface. The liquid film so formed is laminar and under the influence of gravity it flows downward. As shown in Fig.5, as more amount of steam flow past the cold walls, the condensation rate increases due to heat interactions with the vapor, condensing liquid and the cold walls. Gradually, the liquid film (condensate) entirely blankets the wall surafce throughout the characteristic length of flow. The laminar film thus formed over the wall surface acts as a barrier for further heat interactions. Due to this resistance offered by the liquid film, the condensation heat transfer coefficient tends to decrease along the direction of flow. In must be noted that, larger the temperature difference (ΔT) between cold wall and

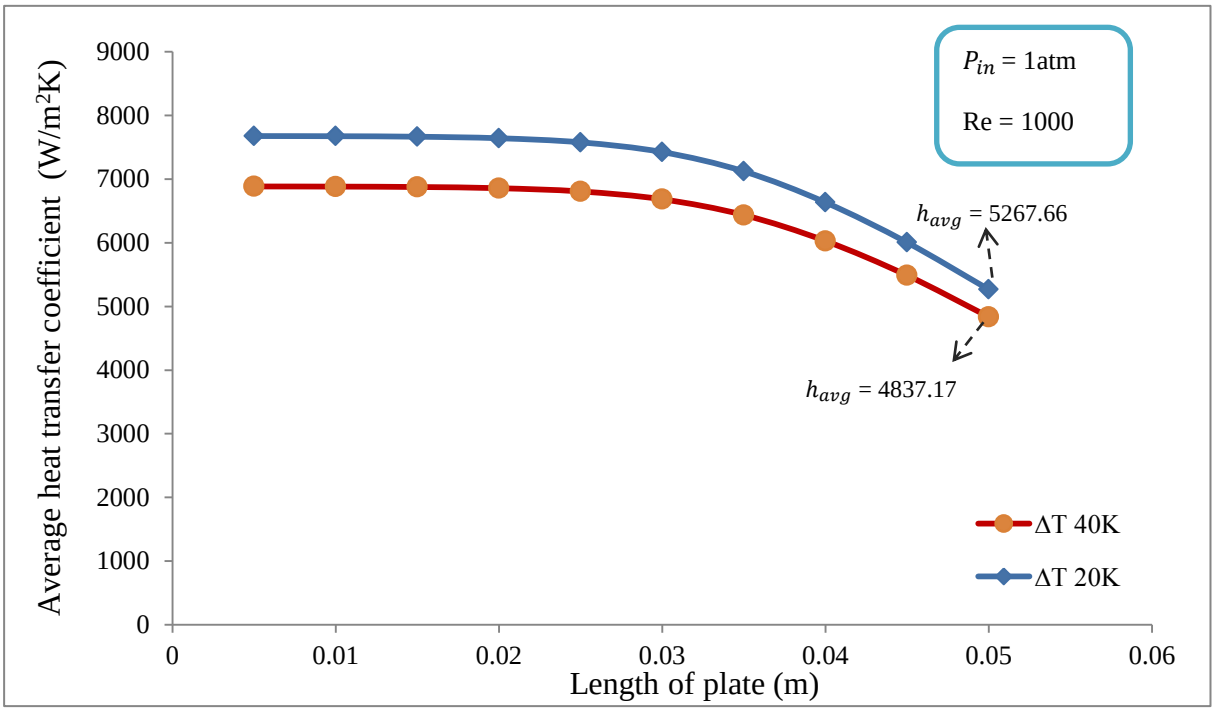

Figure 6. variation of Heat transfer coefficient with ΔT

the incoming vapor greater will be the thermal interaction. Consequently, the liquid film offers a greater resistance and thereby decreases the heat transfer coefficient along the characteristic length. Hence in the Fig. 6, the condensation heat transfer coefficient is higher in magnitude at a temperature difference of ΔT = 20K in comparison with ΔT = 40K.

In Figure 7, the effect of varying values of temperature difference (ΔT) on film thickness or boundary layer thickness is as shown. From the Fig. 7, it can be seen that the formation of boundary layer starts only after a certain distance below the inlet i.e at a distance 0.002m (approx:) from the inlet section. This is because the energy interaction between the cold wall and the incoming vapor becomes appreciable in magnitude only after a certain distance down the inlet favouring condensation. In general we can say that, the thickness of liquid film formed over the surface is inversely propotional to heat transfer coefficient. Thus if larger the magnitude of film thickness lesser will be the heat transfer coefficient. Because thicker film creates a barrier between vapor and the cold wall making it difficult for the vapor to condese on the wall surface. Thus thicker films are formed at a temperature difference of ΔT= 40K in comparison with ΔT= 20K as seen in Fig. 7.

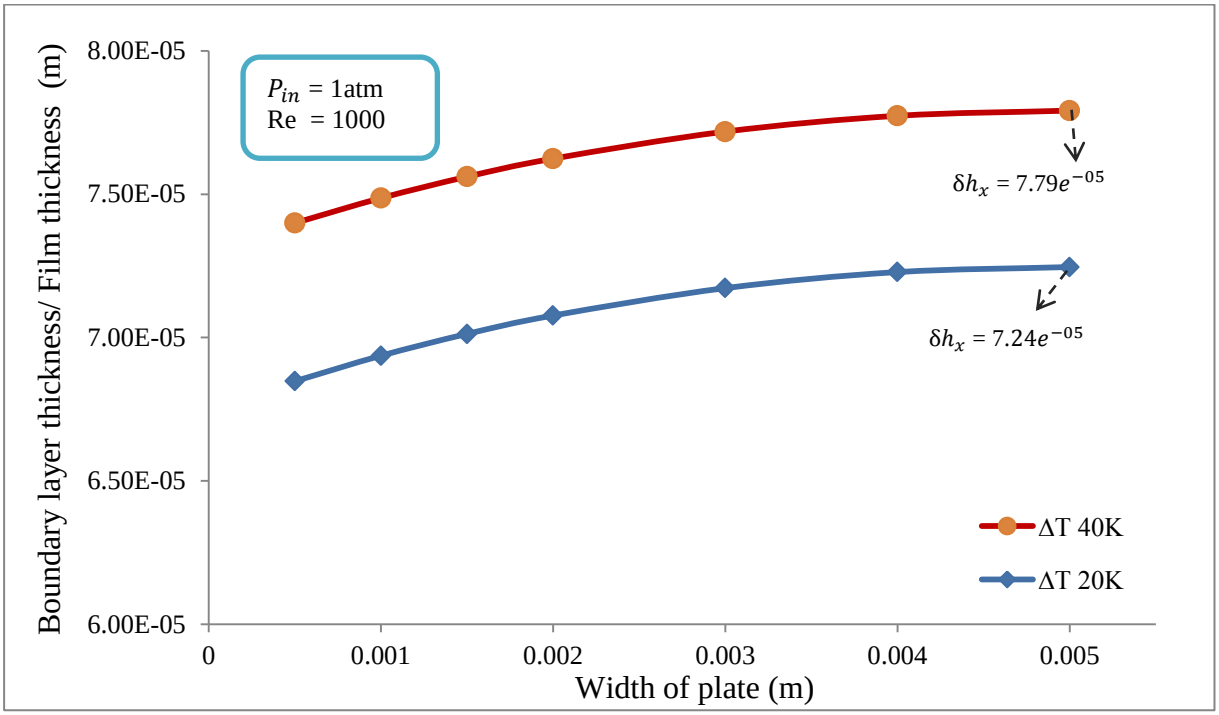

Figure 7. Boundary layer thickness variation with ΔT

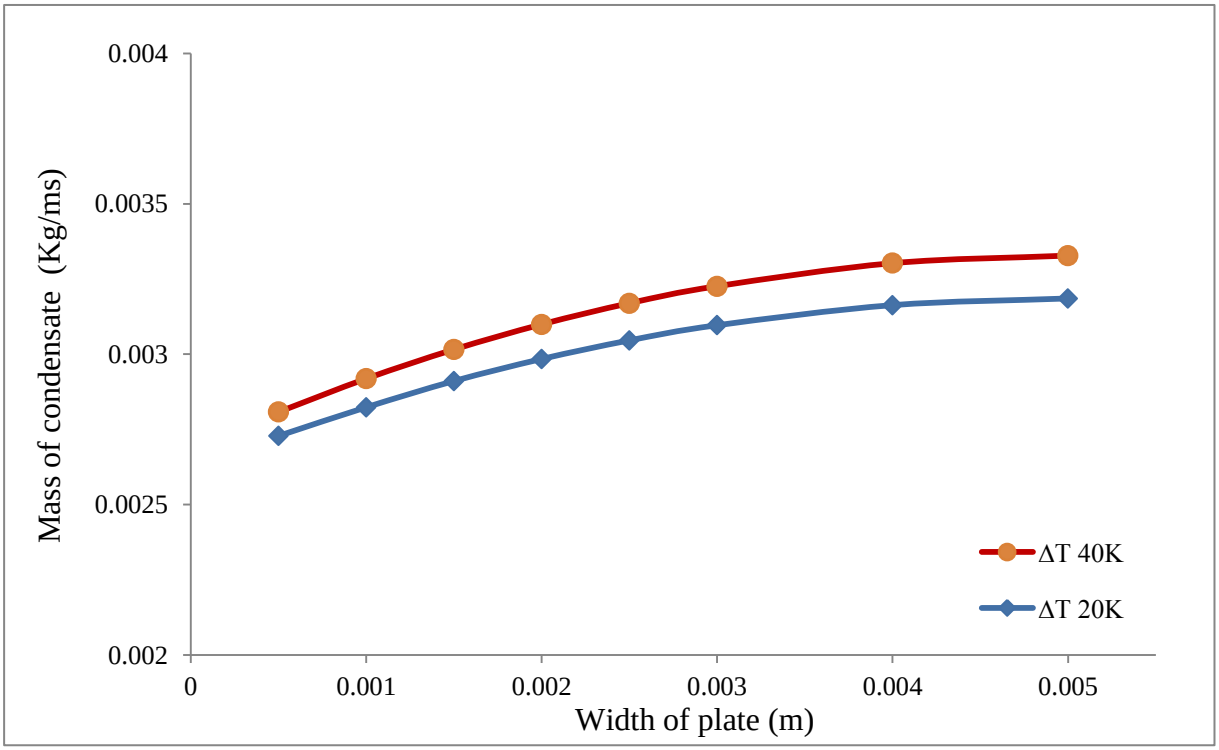

Figure 8. Mass of condensate variation with ΔT

Film thickness can be said to be regarded as a direct parameter to measure the amount of condensate formed on the cold wall surface. In turn, it has dependence on condensing heat transfer coefficient and temperature difference (ΔT). The Eq.10 is used to estimate the mass of condensate formed due to film condensation as a result of heat transfer. Figure 8, depicts the variation of mass of condensate formed at various distances along the plate width for each temperature difference (ΔT). It can be seen from the Fig. 6 and Fig. 7, if larger the heat transfer coefficient lesser will be the film thickness. Hence in Fig. 8, the mass of condensate formed is greater coressponding to a ΔT = 40K when compared to ΔT = 20K closer to the exit end. As mass of condensate formed is lesser near to the inlet, the heat transfer coefficient is larger at the inlet and gradually decreases in the driection of flow.

5. CONCLUSION

In this paper, laminar film condensation was numerically analyzed by developing a solution algorithm using a CFD computation tool, OpenFOAM. The numerical results was verified aganist experimental work of Lee et.al (2015) and it found to be in good agreement with the experimental study. It can be concluded that during film condensation over vertical surfaces, the heat transfer coefficient is influenced by both film thickness and amount of condensate formed over the surface. The plots revealed that as the temperature difference (ΔT) increases, the liquid film thickness formed over the wall surface also increases. With respect to an increase in film thickness, it indicated that the amount of condensate formed over the heat transferring surface also increases. On the other hand, the heat transfer coefficient tends to decrease with an increase in film thickness as the so formed film covers the plate surface and thereby pose a resistance to heat transfer.

Acknowledgement

Authors sincerely acknowledge the support given by Board of Studies in Nuclear Research (BRNS) with the sanction number R/P 2013/36/51 for carrying out this work.

Nomenclature

g	acceleration due to gravity [m s^{-2}]
h_{avg}	average heat transfer coefficient [W m^{-2} K]
h_{fg}	latent heat of vapourization [m^2 s^{-2}]
h	Enthalpy [m^2 s^{-2}]
k	thermal conductivity [W m^{-1} K]
L	characteristic length of flow [m]
$\dot{m}$	mass of condensate formed [kg m^{-1} s^{-1}]
Nu	Nusselt number
p	pressure [N m^{-2}]
p_r	reduced pressure (p/p_c)
Re	Reynolds number
T	temperature [K]
ΔT	temperature difference [K]
ΔT_{wall}	temperature of wall [K]
V	velocity [m s^{-1}]
w	width of plate [m]

Greek symbols

α	alpha (void/phase fraction)
δh_x	film thickness [m]
μ	dynamic viscosity [Pa s^{-1}]
ρ	density [kg m^{-3}]

Subscripts

eff	effective
f	fluid
g	gas phase
in	inlet
L	liquid phase

References

[1] Shah (1979), "A general Correlation for Heat Transfer during film condensation inside pipes", *International Journal of Heat and Mass Transfer*, vol. 22, pp. 547-556

[2] Shah (2009), "An Improved and Extended General Correlation for HT during condensation in Plain Tubes", *American Society of Heating, Refrigerating and Air-Conditioning Engineers, Inc*, vol. 15, No.5, September 2009

[3] S. Thumm, Ch. Philipp & U. Gross (2001), " Film Condensation of water in vertical tubes with Countercurrent vapor flow", *International Journal of Heat and Mass Transfer*, vol. 44, pp. 4245-4256

[4] Xiao-Ze Du & Bu-Xuan Wang (2000), "Study of laminar film-wise condensation for vapor flow in small inclined/ mini-diameter tubes", *International Journal of Heat and Mass Transfer*, vol. 43, pp. 1859-1868

[5] A. S. Dalkilic, S. Yildiz & Wongwises (2009), "Experimental investigation of Convective heat transfer coefficient during downward laminar flow condensation of R-134a in a vertical smooth tube", *International Journal of Heat and Mass Transfer*, vol. 52, pp. 142-150

[6] X. Z. Du & T. S. Zhao (2003), "Analysis of Film Condensation heat transfer inside a vertical micro tube with considerations of the meniscus draining effect", *International Journal of Heat and Mass Transfer*, vol. 46, pp. 4669-4679

[7] Nebuloni Stefano & Thome.R. John, (2010), "Numerical modeling of laminar annular film condensation for different channel shapes", *International Journal of Heat and Mass Transfer*, vol. 53, pp. 2615–2627

[8] Yuwen Zhang & Amir Faghri (2001), "Numerical simulation of condensation on a Capillary Grooved structure", *Numerical Heat transfer*, Part A, vol.39, pp.227-243

[9] Hyoungsoon Lee, Chirag R. Kharangate , Nikhin Mascarehnas, Ilchung Park & Issam Mudawar (2015), "Experimental and computational investigation of vertical down flow condensation", *International Journal of Heat and Mass Transfer*, vol. 85, pp. 865-879

[10] Mimouni.S, Foissac.A & Lavieville.J, (2010), "CFD modeling of wall steam condensation by a two-phase flow approach", *Nuclear Engineering and Design*, vol. 241, pp. 4445–4455

[11] S. Vemuri & K. J. Kim (2005), "An experimental and theoretical study on the concept of dropwise condensation", *International Journal of Heat and Mass Transfer*, vol.49, pp. 649–657

[12] L. Phan & A. Narain (2007), "Nonlinear Stability of classical Nusselt problem of Film condensation and Wave effects", *Journal of Applied Mechanics*, vol. 74, March 2007

[13] C. P Kothandaraman & S. Subramanyan (2010), Heat and Mass transfer Data book (*Seventh Edition*)